Please cite this article in press as: Klattenhoff et al., *Braveheart*, a Long Noncoding RNA Required for Cardiovascular Lineage Commitment, Cell (2013), http://dx.doi.org/10.1016/j.cell.2013.01.003

Cell

Braveheart, a Long Noncoding RNA Required for Cardiovascular Lineage Commitment

Carla A. Klattenhoff,[1,6] Johanna C. Scheuermann,[1,6] Lauren E. Surface,[1] Robert K. Bradley,[1,2,7] Paul A. Fields,[1] Matthew L. Steinhauser,[3] Huiming Ding,[1] Vincent L. Butty,[1] Lillian Torrey,[1] Simon Haas,[1] Ryan Abo,[1] Mohammadsharif Tabebordbar,[1,4,8] Richard T. Lee,[3,5] Christopher B. Burge,[1,2] and Laurie A. Boyer[1,*]
[1]Department of Biology
[2]Program in Computational and Systems Biology
Massachusetts Institute of Technology, 77 Massachusetts Avenue, Cambridge, MA 02139, USA
[3]Division of Cardiovascular Medicine, Department of Medicine, Brigham and Women's Hospital, Harvard Medical School, Partners Research Building, 65 Landsdowne Street, Cambridge, MA 02139, USA
[4]Department of Stem Cells and Developmental Biology, Royan Institute for Stem Cell Biology and Technology, ACECR, Tehran, Iran
[5]Harvard Stem Cell Institute, Cambridge, MA 02138, USA
[6]These authors contributed equally to this work
[7]Present address: Computational Biology Program, Public Health Sciences Division, and Basic Sciences Division, Fred Hutchinson Cancer Research Center, Seattle, WA 98109, USA
[8]Present address: Department of Stem Cell and Regenerative Biology, Harvard University, 7 Divinity Avenue, Cambridge, MA 02138, USA
*Correspondence: lboyer@mit.edu
http://dx.doi.org/10.1016/j.cell.2013.01.003

SUMMARY

Long noncoding RNAs (lncRNAs) are often expressed in a development-specific manner, yet little is known about their roles in lineage commitment. Here, we identified *Braveheart* (*Bvht*), a heart-associated lncRNA in mouse. Using multiple embryonic stem cell (ESC) differentiation strategies, we show that *Bvht* is required for progression of nascent mesoderm toward a cardiac fate. We find that *Bvht* is necessary for activation of a core cardiovascular gene network and functions upstream of mesoderm posterior 1 (*MesP1*), a master regulator of a common multipotent cardiovascular progenitor. We also show that *Bvht* interacts with SUZ12, a component of polycomb-repressive complex 2 (PRC2), during cardiomyocyte differentiation, suggesting that *Bvht* mediates epigenetic regulation of cardiac commitment. Finally, we demonstrate a role for *Bvht* in maintaining cardiac fate in neonatal cardiomyocytes. Together, our work provides evidence for a long noncoding RNA with critical roles in the establishment of the cardiovascular lineage during mammalian development.

INTRODUCTION

The heart is the first organ to function during vertebrate embryogenesis. In mammals, cardiogenesis involves the diversification of pluripotent cells in the embryo toward mesodermal and cardiac cell types, including cardiomyocytes (Kattman et al., 2007). Coordination of this process depends on precise control of gene expression patterns, and disruption of transcriptional networks that govern cardiac commitment underlies congenital heart disease (CHD) (Bruneau, 2008; Srivastava, 2006). Notably, cardiovascular disease and aging lead to a progressive loss of cardiomyocytes, yet the adult mammalian heart has limited regenerative capacity (Mercola et al., 2011; Steinhauser and Lee, 2011). The derivation of cardiomyocytes from pluripotent stem cells in vitro is a potentially promising strategy for regenerative therapy, but the inability to generate sufficient quantities of high-quality cardiac cells has been a limitation to realizing this potential. Thus, knowledge of the molecular switches that control cardiac commitment is critical to achieve a better understanding of heart development and to design better approaches for treatment of cardiac-related diseases.

Development of the cardiovascular system, including the heart, is a multistep process that is coordinated by a network of transcription factors (Murry and Keller, 2008; Olson, 2006). For example, the transcription factor mesoderm posterior 1 (MESP1) is critical for the establishment of a multipotent cardiovascular progenitor population during gastrulation (Bondue et al., 2008; Lindsley et al., 2008). *MesP1* is transiently expressed in the nascent mesoderm, and its expression marks those cells destined to give rise to the cardiovascular lineage (Saga et al., 1996, 1999, 2000). Consistent with this idea, forced expression of *MesP1* during embryonic stem cell (ESC) differentiation leads to an increase in the cardiogenic population (Bondue et al., 2008). MESP1 regulates a core network of transcription factors, including many regulators of heart development as well as genes with roles in epithelial-to-mesenchymal transition (EMT) such as *Snai* and *Twist* (Bondue et al., 2008; Lindsley et al., 2008). EMT is critical for gastrulation and morphogenetic movements during organogenesis, including heart formation (Lim and Thiery, 2012; von Gise and Pu, 2012). Thus, identifying additional factors that promote a mesoderm-to-cardiovascular transition may provide mechanistic insights into the regulation of heart development.

Long noncoding RNAs (lncRNAs) are broadly classified as transcripts longer than 200 nucleotides that are 5′ capped and polyadenylated like most mRNAs, yet this class of transcripts has limited coding potential. lncRNAs function in a wide range of processes and can regulate gene expression by diverse mechanisms (Hu et al., 2012; Mercer et al., 2009; Ponting et al., 2009; Rinn and Chang, 2012). Though thousands of lncRNAs have been identified across eukaryotes, many are species specific and appear less conserved than protein-coding genes (Cabili et al., 2011; Derrien et al., 2012; Ulitsky et al., 2011). Importantly, lncRNAs are differentially expressed across tissues, suggesting that they regulate lineage commitment. Consistent with this idea, loss of function of two lncRNAs in zebrafish embryos, cyrano and megamind, resulted in various developmental defects (Ulitsky et al., 2011). Moreover, HOTTIP plays a role in limb formation (Wang et al., 2011), whereas other lncRNAs function to promote or suppress somatic differentiation (Hu et al., 2011; Kretz et al., 2012a, 2012b). Furthermore, depletion of a subset of lncRNAs in mouse ESCs led to upregulation of global lineage programs (Guttman et al., 2011). Despite these promising findings, our knowledge of lncRNAs that function in lineage commitment is limited to only a few examples, and a detailed understanding of the genetic pathways that they regulate is lacking.

Here, we report the identification of *AK143260*, which we named *Braveheart (Bvht)*, a lncRNA in mouse that is necessary for cardiovascular lineage commitment. Using multiple ESC differentiation strategies, we found that *Bvht* was necessary for activation of a core gene regulatory network that included key cardiac transcription factors (e.g., *MesP1*, *Gata4*, *Hand1*, *Hand2*, *Nkx2.5*, and *Tbx5*) and EMT genes (e.g., *Snai* and *Twist*). Further analysis revealed a significant overlap between the genes regulated by *Bvht* and MESP1, a master regulator of cardiovascular potential. Moreover, forced expression of *MesP1* rescued the *Bvht* depletion phenotype, indicating that these two factors function in a similar genetic pathway. We show that *Bvht* interacts with SUZ12, a core component of polycomb-repressive complex 2 (PRC2), suggesting that this interaction may be critical for epigenetic regulation of network genes. We also demonstrate that *Bvht* is necessary for maintenance of cardiac fate in ex vivo neonatal cardiomyocytes. Together, these results indicate that *Bvht* functions to regulate gene expression programs that promote commitment toward the cardiovascular lineage. More broadly, our work identifies a potential additional pathway for regulation of heart development and suggests that lncRNAs represent targets that can be exploited for efficient generation of stem-cell-derived cardiac cells.

RESULTS

Identification of Candidate lncRNAs in the Cardiac Lineage

lncRNAs exhibit distinct expression patterns across tissues (Derrien et al., 2012; Dinger et al., 2008); however, we have limited knowledge of their precise molecular roles during mammalian development. We reasoned that lncRNAs whose expression becomes restricted to specific cell types during ESC differentiation represent candidate regulators of lineage commitment. We analyzed lncRNA expression as measured by RNA-seq in mouse ESCs as well as in differentiated tissues representing the three germ layers (Mortazavi et al., 2008). We identified 47 candidates that displayed high expression in ESCs and lower median expression across the tissues examined (Figure 1A and Table S1 available online). To identify lncRNAs with potential roles in cardiac commitment, we next evaluated the expression of individual candidates in each tissue, including the heart (Figure 1B). We focused on *AK143260* located on mouse chromosome 18:61,799,307–61,807,126 (+ strand, mm9) because it displayed higher expression in the heart relative to the other tissues examined in this study. Thus, we named the candidate *Braveheart* (*Bvht*).

lncRNAs are a newly emerging class of RNA, and their status as noncoding transcripts from genome annotations requires independent validation. We determined by rapid amplification of cDNA ends (RACE) that *Bvht* is an ~590 nucleotide transcript comprising three exons, consistent with our RNA-seq and northern analysis in ESCs (Figures 1C and 1D). We also detected an isoform that lacked the first exon (~50 bases), which represented only a minor fraction of the total transcript as determined by RACE. Cell fractionation followed by quantitative RT-PCR (qRT-PCR) showed that ~33% of the spliced *Bvht* transcript resides in the nucleus (Figure S1A). Notably, HOTAIR, a lncRNA with nuclear function, is also distributed across both cell compartments in human fibroblasts (Khalil et al., 2009). Though *Bvht* harbors short open reading frames (ORFs) (the two largest are 48 and 74 aa), ORFs of this size would be expected by chance in a transcript of this length (Figure S1B). Consistent with the recent finding that lncRNAs are rarely translated in human cells (Bánfai et al., 2012), we found no evidence of active translation or production of a protein product from *Bvht* (Figures S1C–S1F and Supplemental Information). Moreover, sequence homology searches revealed no clear orthologous *Bvht* sequence or transcripts in syntenic regions of the human or rat genomes, consistent with the idea that lncRNAs are less conserved than protein-coding genes (Cabili et al., 2011; Derrien et al., 2012). For example, analysis of RNA-seq data from human and rat heart, a tissue in mouse that displays strong expression of both *Bvht* and the conserved neighboring *miR143/145* cluster, revealed robust expression of the pri-miRNA in human and rat, whereas transcripts from the *Bvht* region were not detected (Figure 1E). Thus, *Bvht* appears to be a mouse-specific lncRNA and is an example of a recently evolved rapid gain-of-function noncoding transcript.

Braveheart Is Necessary for Proper ESC Differentiation

To dissect the function of *Bvht* in lineage commitment, we generated mouse embryonic stem cell (mESC) lines that stably expressed short hairpin RNAs (shRNA) directed against either exon 2 or 3. We observed significant depletion (~80%) of the transcript in ESCs as measured by qRT-PCR and northern analysis (Figures 2A and 1D). Notably, *Bvht* depletion in ESCs did not affect colony morphology, expression of pluripotency markers, the fraction of apoptotic cells, or cell-cycle kinetics compared to control cells harboring a nontargeting hairpin (Figures 2B

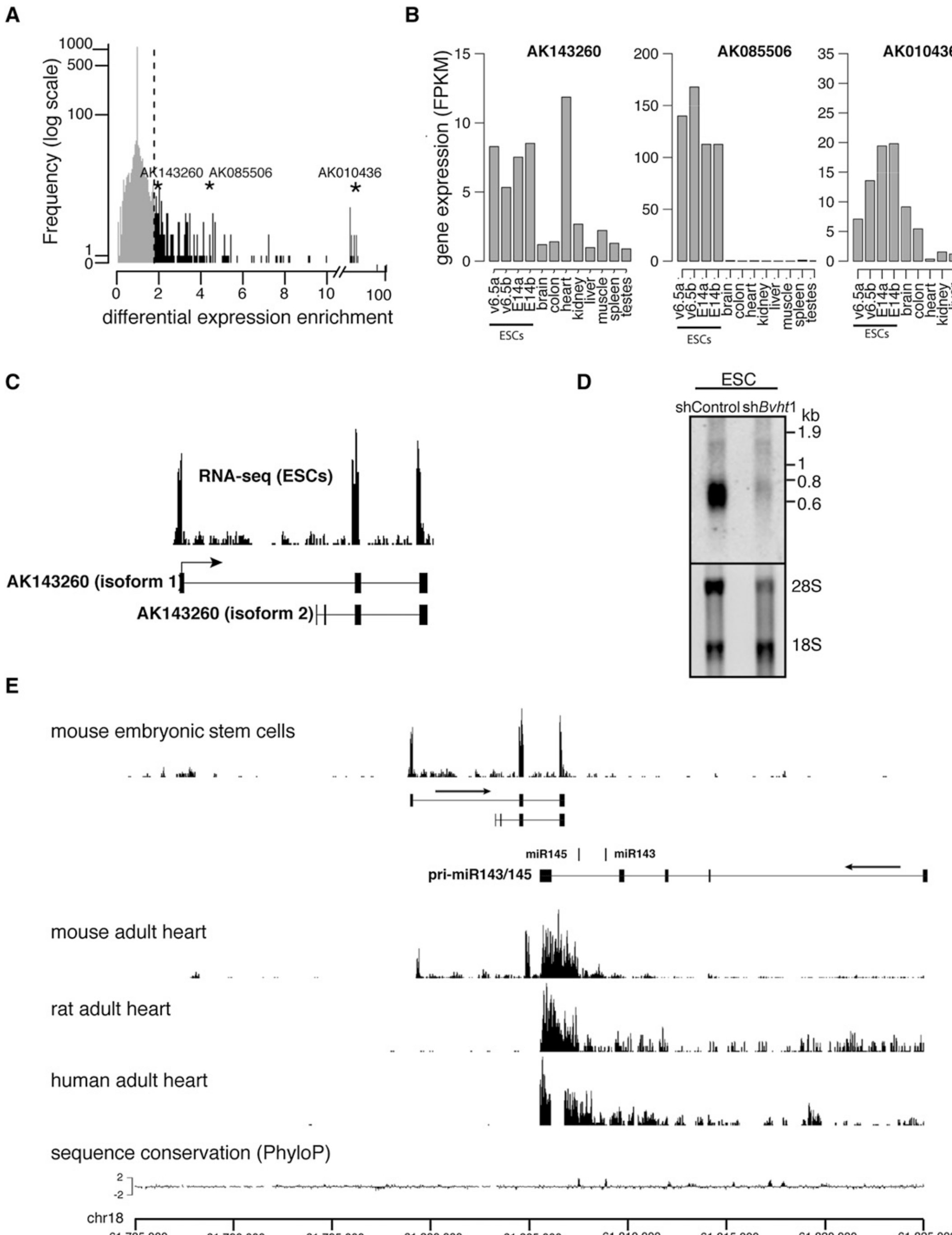

Figure 1. Identification *AK143260* as a Candidate Heart-Associated lncRNA

(A) Differential expression enrichment score calculated from RNA-seq data from biological replicates of two independent mESC lines and adult tissues (brain, liver, and skeletal muscle) representing the three germ layers. Stars represent the position of three example candidates and their respective GenBank accession numbers. The y axis represents the number of lncRNAs with a particular differential expression enrichment, as denoted by each bar.

(B) Transcriptome analysis in a broader range of tissues showed that *AK143260* was predominantly expressed in ESCs and in heart.

(C) Depiction of transcript structure as defined by 5′ and 3′ RACE (bottom) was consistent with RNA sequencing reads in ESCs (top).

(D) Northern analysis using a full-length probe for *AK143260* confirms the predicted size of the transcript (~590 nucleotides) and shows reduced levels upon shRNA-mediated depletion in mESCs.

(E) RNA sequencing reads from rat adult heart and human adult heart samples showed no evidence of a transcript expressed in a location syntenic to *AK143260*. Arrows mark direction of transcription.

See also Figure S1 and Table S1.

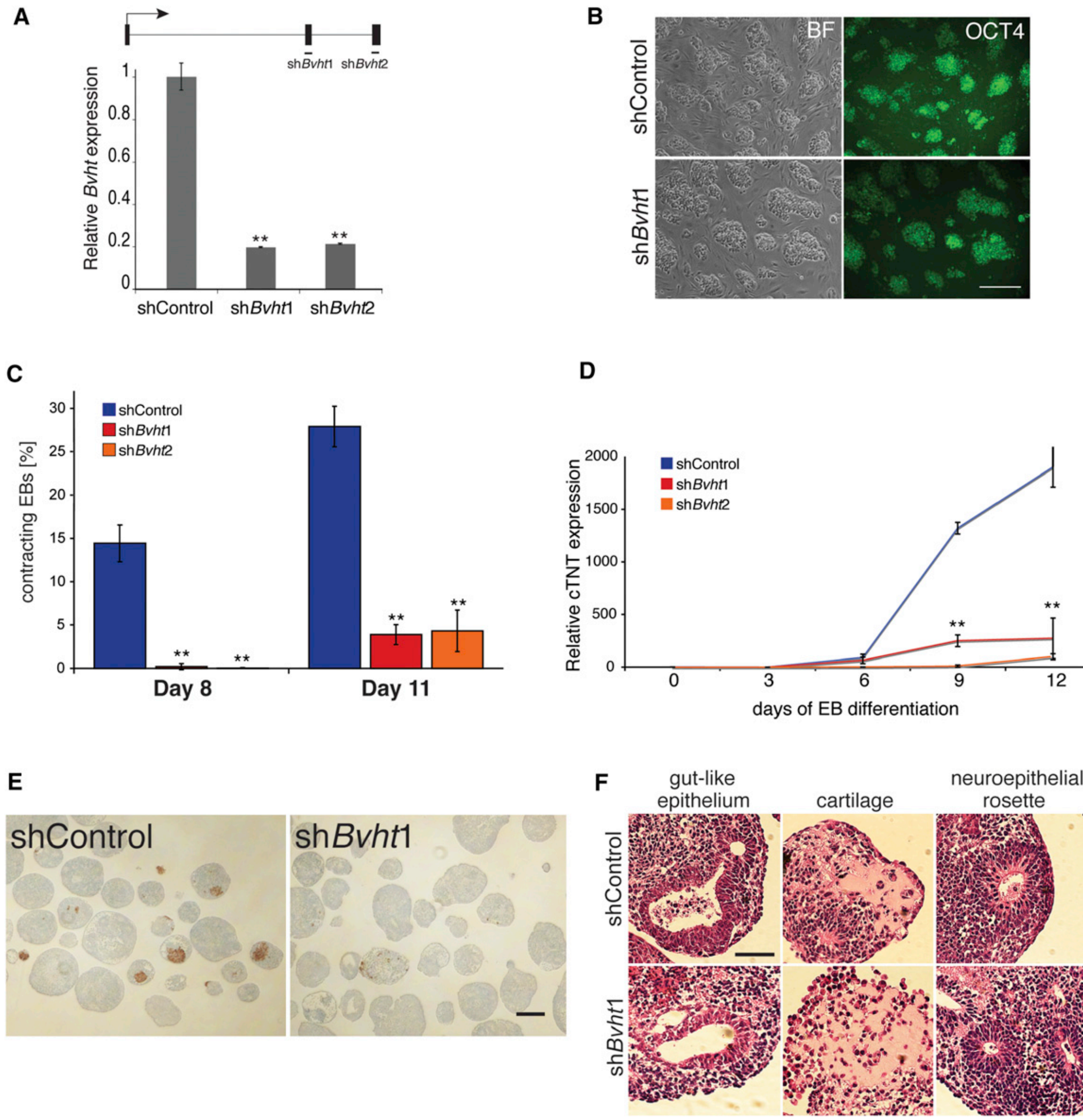

Figure 2. *Bvht* Is Required for Proper ESC Differentiation

(A) Targeting of *AK143260 (Bvht)* in mESCs by two independent hairpins directed to either exon 2 or 3 led to significant depletion of the transcript as measured by qRT-PCR. Experiments were performed in triplicate, and error bars represent SD within one representative experiment.

(B) *Bvht* depletion does not affect colony morphology and OCT4 staining in ESCs. Scale bar, 100 μm.

(C) Percentage of spontaneously contracting EBs determined at days 8 and 11 of differentiation (n > 100 per time point). *Bvht*-depleted EBs showed a significant decrease in contracting EBs compared to controls. The number of resulting EBs was similar in each experiment. Experiments were performed in triplicate, and error bars represent SD.

(D) Expression of cardiac Troponin T (*cTnT*) measured by qRT-PCR at representative time points shows decreased levels in *Bvht*-depleted EBs. Error bars represent SD of a triplicate set of experiments.

(E) Antibody staining of paraffin-embedded sections of day 12 EBs showed decreased cTNT abundance in *Bvht*-depleted compared to controls. Scale bar, 300 μm.

(F) *Bvht*-depleted EBs can form tissues representative of all three germ layers, including gut-like epithelium (endoderm), cartilage (mesoderm), and neuroepithelial rosettes (ectoderm) as represented in hematoxylin and eosin (H&E)-stained EB sections. Scale bar, 100 μm. **$p < 0.01$ by two-tailed Student's t test.

See also Figure S2 and Table S2.

and S2A–S2C). Thus, *Bvht* is not required to maintain ESC self-renewal.

ESCs have the capacity to differentiate into derivatives of the three germ layers, including cardiac cell types. We next induced *Bvht*-depleted ESCs to differentiate by allowing cells to aggregate into embryoid bodies (EBs). Given its expression in the heart, we investigated whether *Bvht*-depleted cells could form cardiac tissue, which can be visualized as spontaneously

Please cite this article in press as: Klattenhoff et al., *Braveheart*, a Long Noncoding RNA Required for Cardiovascular Lineage Commitment, Cell (2013), http://dx.doi.org/10.1016/j.cell.2013.01.003

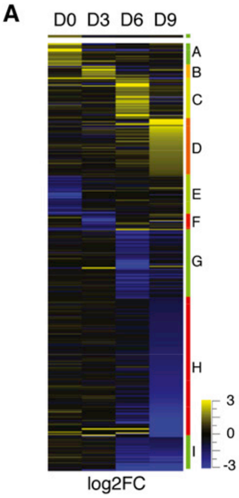

B

Cluster	GO Process	P-value
G	multicellular organismal development	1.65E-24
G	organ morphogenesis	1.22E-09
G	blood vessel development; vasculature development	1.07E-07
G	heart morphogenesis	1.29E-06
G	blood vessel morphogenesis	7.44E-06
H	heart process; heart contraction	1.47E-08
H	actomyosin structure organization	2.46E-08
H	myofibril assembly	2.12E-07
H	muscle system process	5.26E-06
I	multicellular organismal development; developmental process; system development	0.000292
I	oxygen transport	0.0007

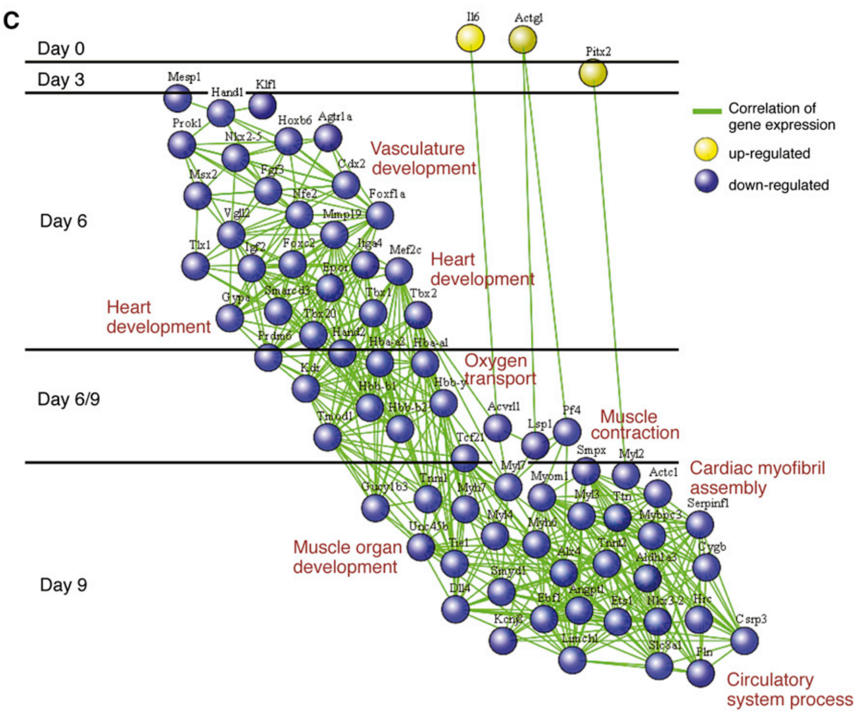

Figure 3. *Bvht* Regulates a Core Network of Genes that Drive Cardiac Differentiation

(A) Heatmap representing hierarchical clustering of all genes that displayed a 3-fold or greater difference in transcript levels in *Bvht*-depleted EBs compared to controls at days 0, 3, 6, and 9.

(B) Significant gene ontology (GO) terms retrieved by clusters G–I.

(C) Pearson correlation network of the EB time course generated using the Spring-embedded algorithm in Cytoscape. Genes in enriched GO categories are represented in the network. A sequence of cardiac transcription factors and genes involved in myofibril organization were not induced during EB differentiation in *Bvht*-depleted cells. Nodes represent genes, and connections represent correlation coefficient.

See also Figures S3, S4, and S5 and Table S3.

contracting EBs during differentiation. In control cells, >25% of EBs beat at day 11 of differentiation, compared to ~5% of the *Bvht*-depleted EBs (Figures 2C, S2D, and S2E). Consistent with this observation, cardiac troponin T (*cTnT*), an integral component of the contraction machinery in cardiac muscle, was expressed at significantly lower levels in *Bvht*-depleted EBs (Figures 2D and 2E). In contrast, cells depleted of *AK085506*, an ESC-specific lncRNA not expressed in the heart, displayed a similar proportion of contracting EBs (Figures 1B and S2F). Examination of EB sections at day 12 of differentiation showed a range of tissues, such as neural rosettes, gut endoderm, and cartilage (Figure 2F). Together, these data suggest that *Bvht* is not required for global ESC differentiation and may have specific functions in cardiac commitment.

***Braveheart* Regulates the Core Cardiovascular Gene Network**

lncRNAs can act in *cis* to regulate expression of neighboring genes or in *trans* by diverse mechanisms (Ørom and Shiekhattar, 2011; Rinn and Chang, 2012). We first analyzed the expression of neighboring genes within a 100 kb window, which included the convergent and overlapping *miR143/145* cluster on the opposite strand (exons do not overlap) (Figure S3A). Expression of neighboring protein-coding genes was unaffected in *Bvht*-depleted cells during ESC differentiation compared to control cells; however, the pri-miRNA was not properly expressed during the time course (Figure S3B). It is likely that lack of expression of the pri-miRNA is due to depletion of cardiac cells in the *Bvht*-depleted EBs rather than direct regulation by *Bvht*. For example, *miR143* and *miR145* are typically transcribed in cardiovascular cell types (Cordes et al., 2009; Xin et al., 2009). Moreover, miR143/145 knockout ESCs formed contracting, cTNT-positive EBs and showed clear differences in gene expression patterns compared to *Bvht*-depleted cells (Figures S3C–S3E and S4 and Table S2). Thus, these data indicate that the *Bvht* phenotype is likely not a consequence of failure to regulate closely neighboring genes in *cis*, including the mir143/145 cluster.

We next reasoned that analysis of global gene expression patterns during EB differentiation might reveal further clues toward elucidating *Bvht* function. To this end, we analyzed gene expression patterns at various time points by RNA-seq. We found ~548 differentially expressed genes in the *Bvht*-depleted cells compared to controls (Figure 3A and Table S3). These genes were clustered by expression pattern, yielding several distinct clusters. Strikingly, genes in clusters that displayed lower expression at later stages (i.e., clusters G–I) showed enrichment for genes that function in heart and blood vessel morphogenesis, heart and muscle system process, and myofibril assembly (Figure 3B). In contrast, genes in clusters that displayed higher expression in *Bvht*-depleted cells (i.e., clusters A–F) were not enriched for specific gene ontology (GO) terms.

To gain further insights, we created a network diagram to illustrate how genes in the enriched GO categories changed in expression over time by computing a Pearson correlation coefficient of expression between all pairs of genes (Figure 3C). Our analysis revealed a complex network of transcription factors that failed to activate during differentiation, including key regulators of heart development, such as *MesP1*, *Hand1*, *Hand2*, *Nkx2.5*, and *Tbx20* as well as genes with roles in cardiomyocyte structure and function, which have been implicated in cardiovascular diseases (Bruneau, 2008; McCulley and Black, 2012). Though a caveat of the EB assay is that it is difficult to distinguish subtle effects among related lineages, we observed that, whereas expression of genes representing cardiovascular cell types, including cardiomyocytes, vascular endothelium, and smooth muscle, were significantly reduced, markers of paraxial mesoderm, hematopoiesis, and endoderm were expressed at normal or slightly elevated levels in *Bvht*-depleted EBs (Figure S5A). Moreover, *Bvht*-depleted cells displayed similar morphology upon neuronal differentiation by addition of retinoic acid and expressed similar levels of neural markers such as *Sox1* and *Nestin* compared to controls (Figure S5B and data not shown). Together, these data suggest that *Bvht* specifically promotes activation of a core gene regulatory network in *trans* to direct cardiovascular cell fate.

Braveheart Functions Upstream of MesP1

MESP1 was among the earliest transcription factors in the gene network that showed significantly lower expression in *Bvht*-depleted EBs. *MesP1* marks a common multipotent cardiovascular progenitor that ultimately specifies all cell types of the heart (Bondue et al., 2008; 2011; David et al., 2008; Lindsley et al., 2008). To test whether *Bvht* and *MesP1* function in a similar pathway, we compared the differentially expressed genes in our EB time course with those changed upon *MesP1* induction (Bondue et al., 2008). We observed a striking correlation among genes that showed lower expression in *Bvht*-depleted cells and higher expression upon *MesP1* induction, denoted as group II ($p < 6 \times 10^{-62}$). Genes that showed higher expression in *Bvht*-depleted cells and reduced expression upon *MesP1* induction also overlapped significantly and were denoted as group III ($p < 9 \times 10^{-45}$) (Figures 4A and 4B). Notably, group II genes function in transcriptional regulation, heart development, and tissue morphogenesis and included many of the transcription factors represented in the *Bvht* network (Figure 4C and Table S4). These results suggest that *Bvht* depletion leads to failure to activate a MESP1-driven gene expression program.

We expected that, if *Bvht* functions upstream of *MesP1*, then forced expression of *MesP1* should rescue the depletion phenotype. We employed a doxycycline-inducible *MesP1* mESC line (Bondue et al., 2008) and induced expression at day 2 of EB differentiation in *Bvht*-depleted and control cells. *MesP1* cardiovascular progenitors comprise a very small proportion of cell types in early stage EBs, and induction at this time point leads to expansion of the cardiogenic population (Bondue et al., 2008; Lindsley et al., 2008). Notably, *MesP1* induction led to an increase in contracting EBs in both control and *Bvht*-depleted cells (Figure 4D). We also found that *Bvht* levels were ~10-fold higher in MESP1 population compared to negative cells using a mESC line that harbored *GFP* under the control of the MesP1 promoter (Bondue et al., 2011) (Figure 4E). Together, these data suggest that *Bvht* functions upstream of *MesP1* as a potential regulator of cardiovascular fate.

Braveheart Promotes Cardiac Cell Fate from Nascent Mesoderm

To further dissect *Bvht* function in the cardiovascular lineage, we employed a directed in vitro cardiomyocyte (CM) differentiation assay that permits isolation of cell populations at well-defined stages (ESCs, precardiac mesoderm [MES], cardiac progenitors [CPs], and CMs) (Kattman et al., 2011; Wamstad et al., 2012) (Figure 5A). Using this assay, we observed that *Bvht*-depleted EBs were smaller and displayed an irregular shape at day 4 (MES) and failed to form an adherent monolayer at day 5.3 (CP) compared to controls (Figure 5B, middle and right panels). In contrast, no visible change in morphology was apparent at day 2, a time point that precedes the addition of cardiac growth factors (Figure 5B, left). We also found an increase in apoptosis but no change in cell-cycle kinetics at day 4 in *Bvht*-depleted cells, whereas day 2 cells showed no difference (Figures 5C and S6A). Notably, shRNA-mediated depletion of *MesP1* showed similar effects to *Bvht* depletion, and *Bvht* overexpression led to an increase in the levels of cardiac genes, including *MesP1*, during CM differentiation (Figures S6B and S6C and data not shown).

Brachyury (*T*) and *Eomesodermin* (*Eomes*), transcription factors expressed in the primitive streak, have critical roles in mesoderm induction and regulate *MesP1* expression by directly binding to its promoter (Costello et al., 2011; David et al., 2011). Though *T* and *Eomes* were expressed normally or at elevated levels at day 4 in *Bvht*-depleted and controls cells, both factors displayed higher levels in day 5.3 *Bvht*-depleted cells (Figure 5D). Notably, expression of core cardiac transcription factors, including MesP1, failed to induce at day 4 and day 5.3 in *Bvht*-depleted cells despite expression of *T* and *Eomes* (Figures 5E and 5F). Similarly, expression of cell surface markers of early cardiac identity (i.e., *PdgfRa* and *Flk-1*) was lower in *Bvht*-depleted cells (Figure 5G). Together, *PdgfRa* and *Flk-1* define an early multipotent cardiovascular progenitor population (marked by *MesP1*), and their coexpression enhances cardiogenic potential (Kattman et al., 2006; Yang et al., 2008). Conversely, *Fgf8* and *Mixl1* levels were elevated in *Bvht*-depleted cells during CM differentiation, consistent with a reciprocal increase in hematopoietic markers upon loss of cardiac potential (Lim et al., 2009; Simões et al., 2011) (Figure S6D).

MESP1 also regulates EMT genes whose expression is critical for migration of precardiac cells during gastrulation (Lindsley et al., 2008). We found that expression of EMT genes such as *Snai1* and *Snai2*, as well as *Twist1* and *Twist2* (Yang et al., 2004), was not induced at day 5.3 in *Bvht*-depleted cells

A

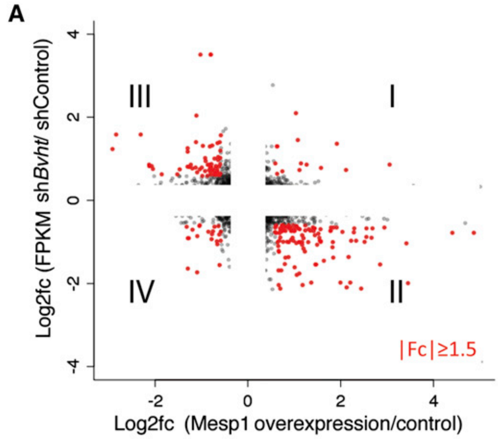

B

Quadrant	Number of overlapping genes	Probability
I	14	0.25
II	115	6.13 E-62
III	67	9.52 E-45
IV	21	0.003

C

Quadrant II GO terms	Enrich.	BenjH
Skeletal system development	8.2	2.5 E-5
Transcription regulation	3.9	2.4 E-4
DNA binding	2.9	3.7 E-3
Tube development	5.8	3.7 E-3
Heart development	5.7	7.4 E-3
Tissue morphogenesis	5.9	6.7 E-3

D

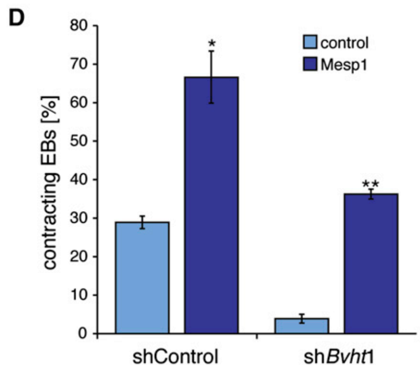

E

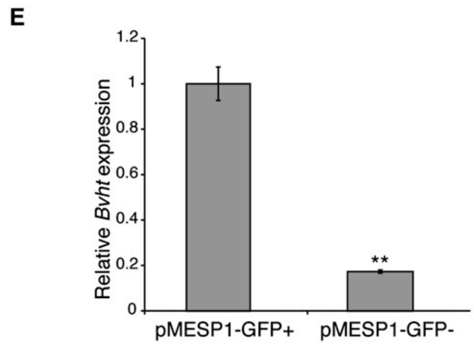

Figure 4. *Bvht* Functions Upstream of *MesP1*

(A) Gene expression comparison between *Bvht* depletion and *Mesp1* induction.

(B) The overlap is highly significant for quadrants II and III as measured by hypergeometric test with Benjamini correction. Genes in quadrant II failed to activate in *Bvht*-depleted cells and are expressed at higher levels upon *Mesp1* induction, whereas quadrant III genes displayed the opposite expression pattern.

(C) Enriched GO terms based on genes in quadrant II.

(D) Forced *MesP1* expression can rescue the contraction defect in *Bvht*-depleted EBs. Contracting EBs were counted at day 11 (n > 100).

(E) *Bvht* is enriched in cells expressing a GFP reporter under the control of the Mesp1 promoter (pMESP1-GFP) compared to GFP-negative cells as analyzed by FACS at day 5 (peak of *MesP1* expression) of EB differentiation followed by qRT-PCR.

Experiments were performed in triplicate, and error bars represent SD in all panels. **p < 0.01 and *p < 0.05 by two-tailed Student's t test. See also Table S4.

compared to controls (Figure 5H). *Snai1* and *Snai2* repress *E-cadherin*, and the switch from *E-cadherin* to *N-cadherin* expression is a hallmark of EMT (Lim and Thiery, 2012). Notably, *E-cadherin* levels remained high, and *N-cadherin* was not expressed in *Bvht*-depleted cells (Figure 5H). Together, these results indicate that *Bvht* is required at a critical time during differentiation when cardiac cells are specified from nascent mesoderm.

Our observations suggest that *Bvht* functions in the same pathway as *MesP1* in a cell-autonomous manner to regulate a core cardiac gene network. To test this idea, we generated ESC lines that harbored either the shBvht or shControl vector additionally marked with GFP or mCherry to allow us to track each population. Equal numbers of shControl-mCherry and shBvht-GFP ESCs were combined and analyzed by fluorescence-activated cell sorting FACS during CM differentiation. Although the proportion of marked cells was similar in ESCs and at day 2, we observed a dramatic overrepresentation of shControl cells at days 4 and 5.3, indicating that *Bvht*-depleted cells cannot efficiently contribute to cardiac cell types (Figure 5I). Similar results were obtained using reciprocal markers (Figure S6E). Notably, cardiac genes such as *Gata4*, *Nkx2.5*, *Tbx5*, and *Isl1* were expressed at normal levels at day 5.3 (Figure S6F), indicating that control cells could differentiate properly in the presence of *Bvht*-depleted cells. Thus, our results support a cell-autonomous role for *Bvht* in the transcriptional control of cardiac cell fate.

Braveheart Interacts with SUZ12, a Core Component of PRC2

Some lncRNAs are thought to act through RNA-protein interactions to effect gene expression by diverse mechanisms (Rinn and Chang, 2012). Because T and EOMES have been shown to bind to the *MesP1* promoter and to regulate its expression (David et al., 2011; Costello et al., 2011), we first tested whether *Bvht* interacted with T or EOMES to mediate their binding at the MesP1 promoter. We performed RNA immunoprecipitation (RIP) using antibodies against T or EOMES; however, we failed to detect

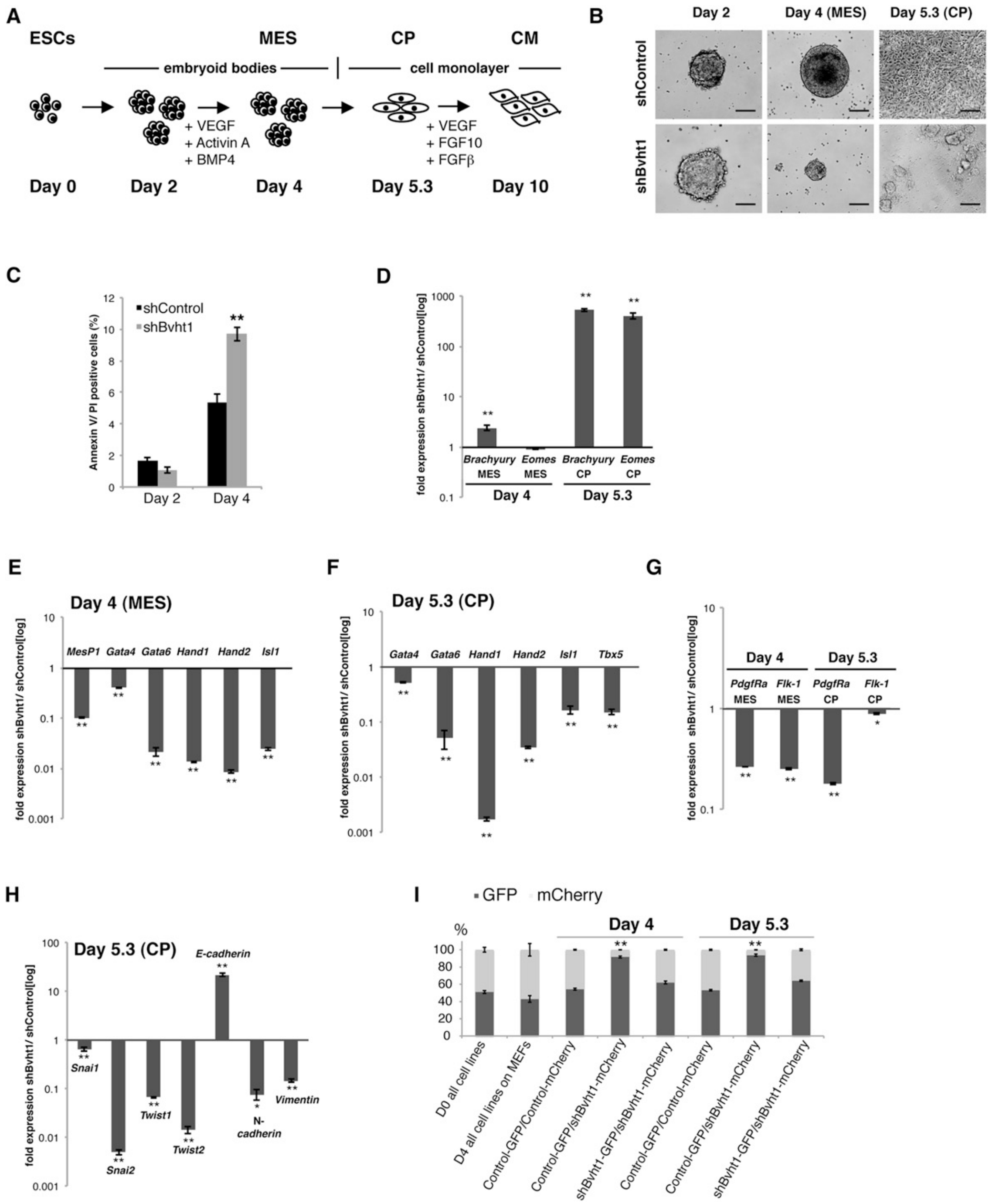

Figure 5. *Bvht* Is Necessary for the Transition from Nascent to Cardiac Mesoderm In Vitro

(A) ESCs were differentiated into beating cardiomyocytes (CM) and progress through precardiac mesoderm (MES) and cardiac progenitor (CP) stages by sequential addition of cytokines.

(B) *Bvht*-depleted EBs were smaller than controls at day 4 and failed to attach and organize into a monolayer at day 5.3. Scale bar, 65 μm.

(C) *Bvht*-depleted cells showed increased levels of apoptosis at day 4 as indicated by quantification of annexin-V-positive cells, whereas no significant difference was observed at day 2.

(D) *Brachyury* and *Eomes* levels remained high at day 5.3 compared to control as measured by qRT-PCR.

(E and F) Core cardiac transcription factors displayed lower expression at days 4 (E) and 5.3 (F) in *Bvht*-depleted cells compared to control.

(G) Expression of cell surface markers *PdgfRa* and *Flk-1* was significantly decreased upon *Bvht* depletion at days 4 and 5.3 compared to control.

(H) EMT genes displayed altered expression patterns in *Bvht*-depleted cells at day 5.3 as measured by qRT-PCR. Values for shControl samples were normalized to 1 for each individual time point.

(legend continued on next page)

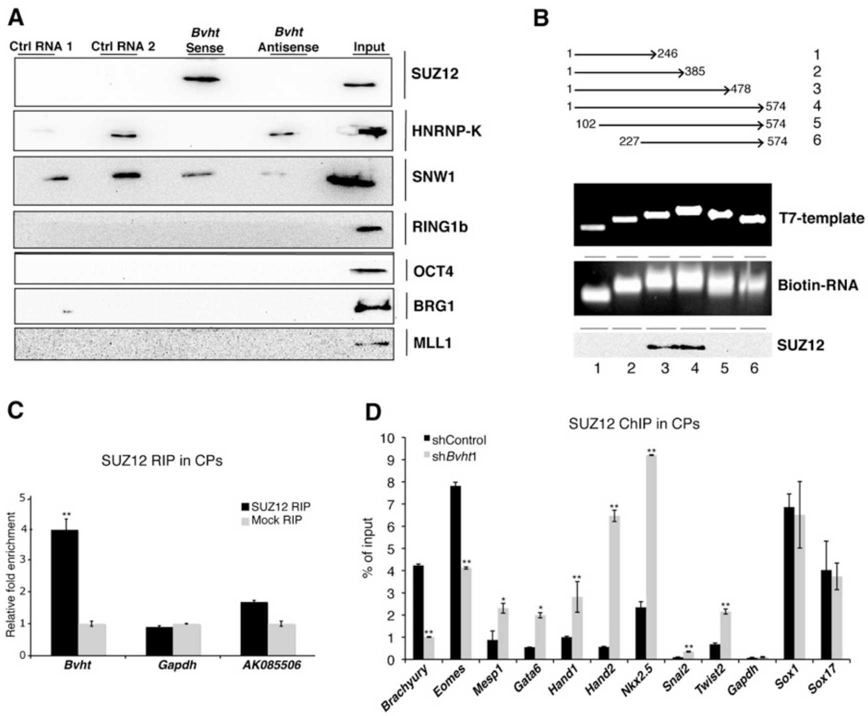

Figure 6. *Bvht* Directly Interacts with SUZ12 during CM Differentiation

(A) Biotin-RNA pull-downs using full-length *Bvht* transcript in nuclear ESC extracts showed specific binding to SUZ12.

(B) Deletion analysis of *Bvht* transcript showed that 5′ and 3′ regions were required for interaction with SUZ12.

(C) *Bvht* interacts with SUZ12 in day 5.3 cells (CP stage) as determined by RIP using SUZ12 antibody.

(D) ChIP using SUZ12 antibody showed higher levels at promoter regions of cardiac and EMT genes in *Bvht*-depleted day 5.3 cells compared to controls, whereas no significant changes were observed in genes expressed in other lineages (e.g., Sox1 and Sox17).

Experiments were performed in triplicate, and error bars represent SD in all panels. $^{**}p < 0.01$ and $^{*}p < 0.05$ by two-tailed Student's t test. See also Figure S7.

a specific interaction with *Bvht* (Figure S7A). We also did not detect changes in the binding of T to the *MesP1* promoter by chromatin immunoprecipitation (ChIP) followed by qPCR (Figure S7B and Supplemental Information). Thus, it is unlikely that *Bvht* directly regulates T or EOMES to control *MesP1* activation.

lncRNAs can act as molecular scaffolds by interacting with chromatin-modifying complexes (Guttman et al., 2011; Tsai et al., 2010). Using in vitro biotin-RNA pull-down, we detected a specific interaction between *Bvht* and SUZ12 in ESCs; however, other factors thought to bind lncRNAs, including hnRNPK, SNW1, RING1b, OCT4, BRG1, and MLL1, did not show a specific interaction (Figure 6A). These data were confirmed by RIP using SUZ12-specific antibodies (data not shown). SUZ12 is a core subunit of PRC2, a complex that catalyzes trimethylation of histone H3 lysine 27 (H3K27me3) and mediates transcriptional repression (Surface et al., 2010). A number of lncRNAs have been shown to interact with PRC2 to regulate target gene expression (Wang and Chang, 2011). We then constructed a series of *Bvht* deletions and found several regions of the transcript that were required for this interaction (Figure 6B), suggesting that *Bvht* directly interacts with PRC2.

Next, we tested whether *Bvht* interacted with SUZ12 during CM differentiation. Similar to ESCs, we found that SUZ12 interacted with *Bvht* by RIP at day 5.3 cells (Figure 6C). We chose to analyze day 5.3 cells because these cells comprise a largely homogenous population of >70% NKX2.5-positive cells and because *Bvht* is enriched in this population (Figure S7C). Many of the cardiac genes that failed to activate in *Bvht*-depleted cells at day 5.3 are known polycomb targets in ESCs (Boyer et al., 2006). These genes are poised for activation in ESCs, as indicated by their bivalent chromatin marks (H3K27me3 and H3K4me3) (Bernstein et al., 2006), and differentiation toward specific lineages requires the selective loss of PRC2 at subsets of genes. We found that, in *Bvht*-depleted cells, SUZ12 levels remained high at the promoters of critical genes in the cardiovascular network, including *MesP1*, *Gata6*, *Hand1*, *Hand2*, and *Nkx2.5*, compared to control cells as measured by ChIP-qPCR (Figure 6D). In contrast, SUZ12 levels were lower at *T* and *Eomes*, consistent with their higher expression at day 5.3 in *Bvht*-depleted cells. SUZ12 levels were equivalent in both *Bvht*-depleted and control cells (Figure S7D). We also found that H3K27me3 levels paralleled SUZ12 enrichment in both *Bvht*-depleted and control cells. Notably, cardiac genes maintained their bivalent status at day 5.3 (Figures S7E and S7F), consistent with a failure to activate the cardiac program. Though our data do not distinguish between a direct or indirect mechanism, these results along with the demonstrated interaction between SUZ12 and *Bvht* suggest that *Bvht* functions, in part, with PRC2 to regulate cardiac commitment.

Braveheart Is Necessary for Maintenance of Cardiac Fate in Neonatal CMs

Our data show that *Bvht* is required for the commitment of ESCs toward a cardiac fate. Because we detected expression of *Bvht* in the adult mouse heart (Figure 1B), we investigated whether *Bvht* functions in later stages of differentiation. We

(I) Equal numbers of mCherry-shControl and GFP-sh*Bvht1* cells were mixed and subjected to cardiac differentiation. A dramatic decrease in *Bvht*-depleted cells was observed at days 4 and 5.3, whereas cells cultured in ESC conditions maintain equal distribution.

Error bars represent SD of three replicates within one representative experiment. $^{**}p < 0.01$ and $^{*}p < 0.05$ by two-tailed Student's t test. See also Figure S6.

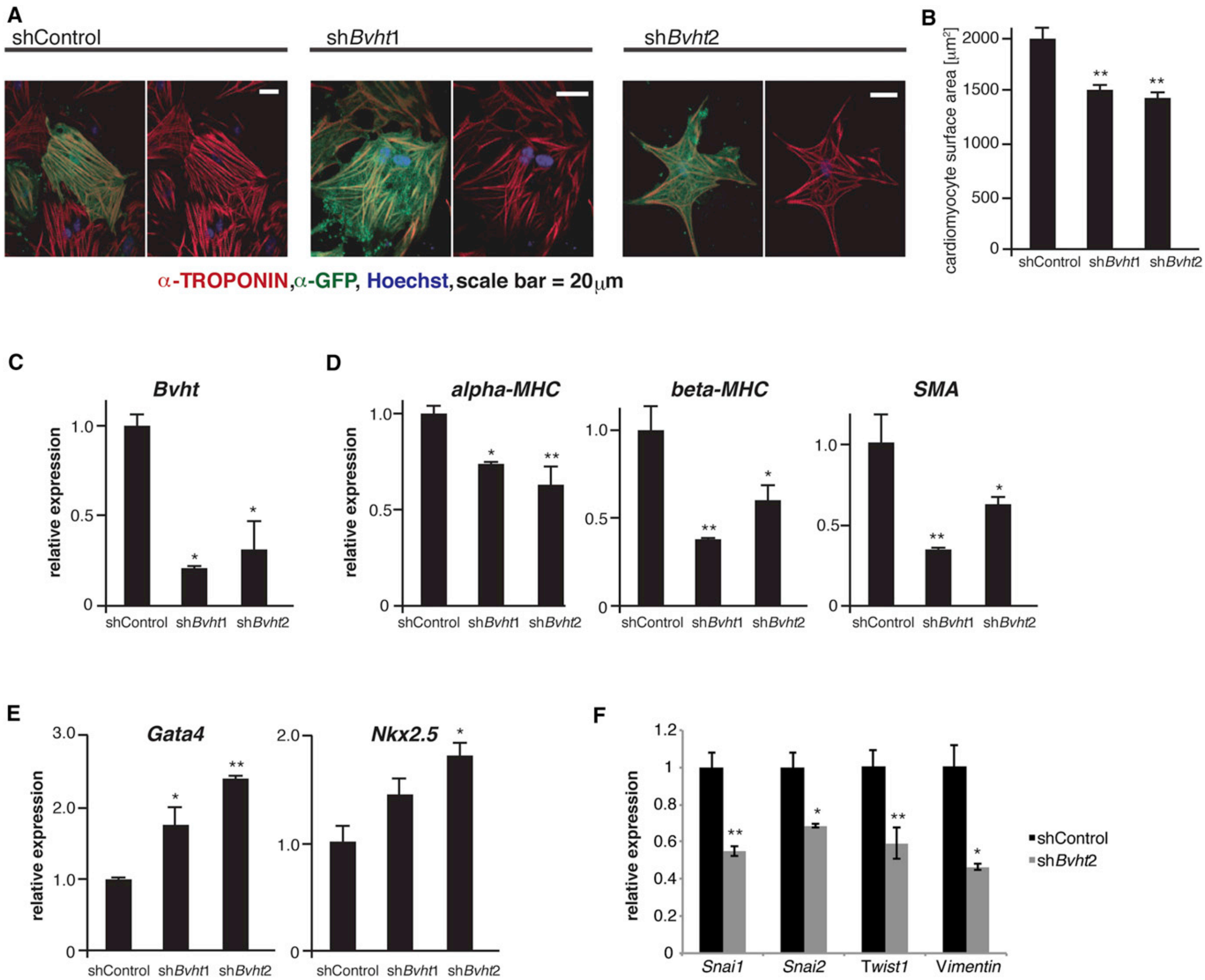

Figure 7. *Bvht* Is Required to Maintain Cardiac Fate in Neonatal Cardiomyocytes

(A) *Bvht*-depleted or control nCMs were identified by the presence of a GFP reporter in the shRNA vector. Myofibrils clustered together in GFP-positive control cells, whereas *Bvht* depletion resulted in disorganized cardiac myofibril bundles. Myofibrils were visualized by IF using an antibody against cTnT (red) and GFP (green). Nuclei (blue) were stained with Hoechst. Scale bars, 20 μm.

(B) *Bvht*-depleted nCMs were overall smaller than controls as assessed by the surface area of GFP-positive versus control cells ($n > 100$).

(C) Global levels of *Bvht* (qRT-PCR) in control and *Bvht*-depleted nCM cultures.

(D) Reduced expression of sarcomeric and myofibril components in *Bvht*-depleted nCMs as measured by qRT-PCR.

(E) Expression (qRT-PCR) of transcription factors involved in early cardiogenesis was increased in *Bvht*-depleted cells.

(F) Factors involved in EMT were expressed at lower levels in *Bvht*-depleted cells.

Experiments were performed in triplicate, and error bars represent SD in all panels. **$p < 0.01$ and *$p < 0.05$ by ANOVA and Dunnett's test.

analyzed the effect of *Bvht* depletion in primary murine neonatal ventricular cardiomyocyte (nCMs) cultures, a model that has been used extensively for investigating drug and injury responses (Louch et al., 2011). In brief, nCMs were isolated from the newborn heart, a stage when myocytes display plasticity both in vivo and in vitro, as evidenced by increased levels of early cardiac markers such as *Gata4* and *Nkx2.5* (Porrello et al., 2011; Zhang et al., 2010). Within days of isolation, nCMs are able to organize into myofibrils, forming sheets of beating cardiomyocytes in explant cultures. Thus, neonatal cardiomyocytes represent an ex vivo model in which to test the role of *Bvht* in modulating cardiac cell fate in the heart.

nCMs were infected 1 day after explant with *Bvht* or control shRNA lentiviruses harboring a GFP marker. We found that *Bvht*-depleted nCMs as marked by GFP displayed unevenly distributed and irregularly bundled myofibrils after 5 days in culture compared to control cells as evidenced by cTNT staining (Figure 7A). Consistent with this observation, the overall cell surface area of individual GFP-positive nCMs was significantly smaller (Figure 7B), indicating that nCM structure is disrupted in *Bvht*-depleted cells (Figure 7C). Moreover, structural genes that were not properly activated in *Bvht*-depleted EBs, including α- and β-*MHC* and *Sma*, displayed lower expression in the *Bvht*-depleted nCMs compared to controls (Figure 7D), whereas early cardiac markers *Gata4* and *Nkx2.5* displayed higher expression (Figure 7E). Notably, genes involved in EMT such as *Snai* and *Twist* members, as well as *Vimentin*, showed lower expression in *Bvht*-depleted nCMs (Figure 7F). These data suggest that *Bvht* plays a critical role in promoting cardiac gene expression programs and tissue remodeling in the developing heart.

DISCUSSION

Dynamic regulation of gene expression programs is critical for cell fate transitions during lineage commitment, and faulty regulation can lead to developmental failure and disease. Heart development is a multistep process regulated by a network of transcription factors, and disruption of transcriptional networks leads to congenital heart disease (Bruneau, 2008; McCulley and Black, 2012; Olson, 2006; Srivastava, 2006). Though many of the genetic factors that govern heart development are known, we hypothesized that lncRNAs may represent an additional layer of regulation. Here, we identify *Braveheart* as a critical regulator of cardiovascular commitment from nascent mesoderm, representing the first example of a lncRNA with potential implications in cardiovascular development.

The temporal activation of a core transcription factor network establishes the plan for a primitive heart. The genes in this network are highly conserved during evolution, whereas the formation of more complex and species-specific substructures is likely a consequence of evolution of species-specific regulators. Analysis of sequence conservation and potential transcripts in syntenic regions in the rat and human genomes did not identify a *Bvht* homolog. The lack of conservation is likely due to both weak selective pressure on the primary sequence of lncRNAs and rapid gain and loss of entire lncRNA genes. For example, noncoding genes such as *Xist* and *Neat1* have undergone rapid sequence evolution while preserving their functional roles (Clemson et al., 2009; Nesterova et al., 2001). Increasing evidence also suggests that lncRNAs are largely species specific, with many transcripts arising from the primate lineage (Derrien et al., 2012). Thus, *Bvht* appears to represent a nonconserved lineage-specific lncRNA; however, we expect that other species with a defined circulatory system may have evolved lncRNAs with similar functions.

Bvht Is an Upstream Regulator of Cardiovascular Commitment

Our work suggests that *Bvht* functions upstream of and in the same genetic pathway as *MesP1* as a permissive factor for cardiac commitment during ESC differentiation. *MesP1* expression can specify all cell types of the cardiovascular lineage (Bondue et al., 2008; Lindsley et al., 2008), and its expression is sufficient to transdifferentiate dermal fibroblasts into cardiac progenitors along with the transcription factor ETS2 (Islas et al., 2012), indicating that *Bvht* may also be critical for forward programming and reprogramming toward a cardiovascular fate. EMT is critical for gastrulation and morphogenetic movements throughout development, including during heart formation (Lim and Thiery, 2012; von Gise and Pu, 2012). EMT is equally critical for in vitro differentiation of stem cells and somatic cell reprogramming, during which cells transition through multiple stages (Esteban et al., 2012). *Snai and Twist*, well-characterized regulators of EMT, are downstream targets of MESP1 and have been implicated in various aspects of heart and vascular development (Lindsley et al., 2008). We found that *Bvht* was necessary for expression of an EMT gene network, including *Snai* and *Twist* members in CM differentiation and in nCMs, indicating that *Bvht* may also regulate cardiac commitment through organization of a functional tissue.

Bvht May Function with PRC2 to Regulate Cardiac Gene Expression Program

Epigenetic regulation plays an important role in development of the cardiovascular system (Chang and Bruneau, 2012). Recent studies have shown that Ezh2, the catalytic component of PRC2, is necessary for repression of the progenitor program during cardiac differentiation and for proper spatiotemporal regulation of cardiac gene expression (Delgado-Olguín et al., 2012; He et al., 2012). We found that *Bvht* directly interacted with PRC2 through SUZ12, a core component of the complex, at several stages during CM differentiation. Notably, SUZ12 and its associated modification H3K27me3 were enriched at promoters of cardiac genes, including MesP1 in *Bvht*-depleted cells. Cardiac genes also remained bivalent in *Bvht*-depleted cells, similar to their configuration in ESCs and consistent with a failure to activate the cardiac program. Although we cannot yet distinguish between a direct or indirect role for *Bvht* at these loci, one model is that *Bvht* binds SUZ12 and competes for PRC2 binding at target sites during the transition from nascent to cardiac mesoderm, leading to activation of the cardiac program. Alternatively, *Bvht* may recruit PRC2 to a repressor of the cardiac program, where loss of *Bvht* would fail to silence the repressor. Though further studies will be required to fully elucidate the mechanism of *Bvht* function, our work suggests that *Bvht* mediates cardiac commitment, in part, by epigenetic regulation of gene expression programs.

Implications of *Bvht* in Cardiovascular Development and Disease

Cardiovascular disease is one of the most common causes of death, yet the mammalian heart has limited regenerative capacity. Thus, a detailed understanding of the pathways involved in cardiogenesis and particularly factors dictating commitment will be instrumental for recapitulating these processes for regenerative therapy. Stem cell models and the generation of specific cell types in vitro offer a potential avenue for studying diseases in a dish and ultimately for transplantation therapy (Burridge et al., 2012). Thus, our finding that *Bvht* is required for progression of cardiac commitment suggests that lncRNAs represent a class of molecular modulators that can direct cell fate. Direct comparisons of cardiovascular-associated lncRNAs across species should contribute further insights into how these regulators are integrated into the gene regulatory networks that drive cardiogenesis and may also provide important clues into the evolution of this complex organ. Moreover, our data suggest that lncRNAs may represent undiscoverd disease loci that, in some cases, may be identifiable by genome-wide association studies (GWAS) (Mattick, 2009; Schonrock et al., 2012). For example, the human lncRNA ANRIL has been associated with a locus implicated in cardiovascular disease (Congrains et al., 2012). In addition, human MIAT was identified as a lncRNA associated with increased risk of myocardial infarction (Ishii et al., 2006). Thus, we anticipate that future studies to identify additional lncRNAs with roles in cardiac function will lead to a better understanding of heart development and will inform strategies for cardiac repair.

EXPERIMENTAL PROCEDURES

Detailed experimental and analysis methods can be found in the Supplemental Information.

ESC Lines and Growth Conditions

E14 (ola/129), V6.5 (SvJae129/C57BL/6), MesP1-GFP, A2lox-MesP1, NKX2.5-GFP, and miR-143/145 ESCs were cultured on irradiated MEFs using standard conditions.

Generation of ESC Lines

shRNA-Mediated Depletion of lncRNAs

shRNAs directed against *Bvht*, *Mesp1*, and control hairpins were cloned into pLKO.1 vector. Production of lentiviral particles and transduction of ESCs was performed according to protocols from The RNAi Consortium (http://www.broadinstitute.org/rnai/trc).

Bvht Overexpression

Full-length Bvht cDNA was cloned into pSLIK vector, and transgenic cells were generated as described above.

ESC Differentiation

Embryoid Body Formation

ESCs were preplated to remove feeders, diluted to 100,000 cells/ml in complete growth medium lacking LIF, and plated on low-attachment cell culture plates.

Cardiomyocyte Differentiation

Directed differentiations and analysis were performed as described (Wamstad et al., 2012).

Identification of Candidate lncRNAs

Expression data from ESCs (V6.5 and E14) (this study) and adult tissues (Mortazavi et al., 2008) were collated using two annotations (Flicek et al., 2011; Guttman et al., 2010) to define a set of murine lncRNAs. Candidate lncRNAs were identified by a stringent set of criteria outlined in the Supplemental Information.

Genomic Analysis of *Braveheart*

5′ and 3′ RACE was performed using FirstChoice RLM-RACE kit (Ambion) on ESC RNA, and products were cloned using TOPO TA cloning kit (Invitrogen). See Table S5 for primer sequences.

Preparation of RNA Sequencing Libraries and Analysis

RNA-seq was performed as described (Wamstad et al., 2012), and reads were mapped using Tophat/Bowtie. Isoform identification and quantification were performed using Cufflinks. RNA-seq quality control metrics are listed in Table S6.

Gene Coexpression Network

The cascade network of coexpression was generated based on the Pearson correlations of the RNA-seq expression profiles, which are described by $\log_2$-fold change between *Bvht* and control knockdown cells. The layout of the network was created using the Spring-Embedded layout algorithm (Cytoscape plug-in), as described in the Extended Experimental Procedures.

Competition Assay/Cell Autonomy

GFP and mCherry coding sequences were cloned into pIKO.1 vector containing control and *Bvht* hairpins (Table S5). Cells were isolated by FACS 4 days after infection to select for those expressing the fluorescent proteins. Equal numbers of ESCs were mixed, analyzed by FACS, and then plated under cardiomyocyte differentiation or ESC culture conditions. Cells were analyzed by FACS at various time points to determine the proportion of each fluorescently marked population.

RNA Immunoprecipitation

Native RIP was performed as described (Rinn et al., 2007). Antibodies are listed in the Supplemental Information.

Chromatin Immunoprecipitation

The ChIP protocol has been adapted from previous studies (Creyghton et al., 2008). Antibodies are listed in the Supplemental Information. ChIP-enriched DNA was quantified by qRT-PCR. Primers are listed in Table S5.

Isolation and Manipulation of Primary Mouse Neonatal Cardiomyocytes

Murine neonatal cardiomyocytes (nCMs) were isolated from C57B6 mice within the first 24 hr after birth. A detailed protocol can be found in the Extended Experimental Procedures.

ACCESSION NUMBERS

All RNA-sequencing data generated during the course of this study, including raw reads and analysis files, have been deposited to GEO under the accession ID GSE39656.

SUPPLEMENTAL INFORMATION

Supplemental Information includes Extended Experimental Procedures, seven figures, and six tables and can be found with this article online at http://dx.doi.org/10.1016/j.cell.2013.01.003.

ACKNOWLEDGMENTS

We thank members of the Boyer lab, especially Sera Thornton, for helpful discussions and critical evaluation of the manuscript and members of the Burge lab, especially Jason Merkin and Jessica Hurt, for sharing unpublished data. We also thank MIT BioMicro Center members Fugen Li, Kevin K. Thai, and Stuart Levine for bioinformatics and technical support. We are especially grateful to Nadya Dimitrova and Tyler Jacks for miR-143/145 conditional KO ESC lines and Cedric Blanpain for inducible MesP1 and pMesP1-GFP reporter ESC lines and for providing gene expression data. R.K.B. was supported by the Damon Runyon Cancer Research Foundation (DRG 2032-09 and DFS 04-12). M.L.S. was supported by NIH K08 (DK090147) and the Watkins Cardiovascular Leadership Award. C.A.K. is a Novartis Scholar of the Life Sciences Research Foundation. J.C.S. is supported by an EMBO long-term fellowship. This work was supported by the NHLBI Bench to Bassinet Program (U01HL098179 and U01HL098188) (L.A.B.); the Richard and Susan Smith Family Foundation, Chestnut Hill, MA (L.A.B.); and the Pew Scholar's Program in the Biomedical Sciences (L.A.B.).

Received: July 26, 2012
Revised: November 9, 2012
Accepted: December 20, 2012
Published: January 24, 2013

REFERENCES

Bánfai, B., Jia, H., Khatun, J., Wood, E., Risk, B., Gundling, W.E., Jr., Kundaje, A., Gunawardena, H.P., Yu, Y., Xie, L., et al. (2012). Long noncoding RNAs are rarely translated in two human cell lines. Genome Res. *22*, 1646–1657.

Bernstein, B.E., Mikkelsen, T.S., Xie, X., Kamal, M., Huebert, D.J., Cuff, J., Fry, B., Meissner, A., Wernig, M., Plath, K., et al. (2006). A bivalent chromatin structure marks key developmental genes in embryonic stem cells. Cell *125*, 315–326.

Bondue, A., Lapouge, G., Paulissen, C., Semeraro, C., Iacovino, M., Kyba, M., and Blanpain, C. (2008). Mesp1 acts as a master regulator of multipotent cardiovascular progenitor specification. Cell Stem Cell *3*, 69–84.

Bondue, A., Tännler, S., Chiapparo, G., Chabab, S., Ramialison, M., Paulissen, C., Beck, B., Harvey, R., and Blanpain, C. (2011). Defining the earliest step of cardiovascular progenitor specification during embryonic stem cell differentiation. J. Cell Biol. *192*, 751–765.

Boyer, L.A., Plath, K., Zeitlinger, J., Brambrink, T., Medeiros, L.A., Lee, T.I., Levine, S.S., Wernig, M., Tajonar, A., Ray, M.K., et al. (2006). Polycomb complexes repress developmental regulators in murine embryonic stem cells. Nature *441*, 349–353.

Bruneau, B.G. (2008). The developmental genetics of congenital heart disease. Nature *451*, 943–948.

Burridge, P.W., Keller, G., Gold, J.D., and Wu, J.C. (2012). Production of de novo cardiomyocytes: human pluripotent stem cell differentiation and direct reprogramming. Cell Stem Cell *10*, 16–28.

Cabili, M.N., Trapnell, C., Goff, L., Koziol, M., Tazon-Vega, B., Regev, A., and Rinn, J.L. (2011). Integrative annotation of human large intergenic noncoding RNAs reveals global properties and specific subclasses. Genes Dev. *25*, 1915–1927.

Chang, C.P., and Bruneau, B.G. (2012). Epigenetics and cardiovascular development. Annu. Rev. Physiol. *74*, 41–68.

Clemson, C.M., Hutchinson, J.N., Sara, S.A., Ensminger, A.W., Fox, A.H., Chess, A., and Lawrence, J.B. (2009). An architectural role for a nuclear noncoding RNA: NEAT1 RNA is essential for the structure of paraspeckles. Mol. Cell *33*, 717–726.

Congrains, A., Kamide, K., Oguro, R., Yasuda, O., Miyata, K., Yamamoto, E., Kawai, T., Kusunoki, H., Yamamoto, H., Takeya, Y., et al. (2012). Genetic variants at the 9p21 locus contribute to atherosclerosis through modulation of ANRIL and CDKN2A/B. Atherosclerosis *220*, 449–455.

Cordes, K.R., Sheehy, N.T., White, M.P., Berry, E.C., Morton, S.U., Muth, A.N., Lee, T.H., Miano, J.M., Ivey, K.N., and Srivastava, D. (2009). miR-145 and miR-143 regulate smooth muscle cell fate and plasticity. Nature *460*, 705–710.

Costello, I., Pimeisl, I.M., Dräger, S., Bikoff, E.K., Robertson, E.J., and Arnold, S.J. (2011). The T-box transcription factor Eomesodermin acts upstream of Mesp1 to specify cardiac mesoderm during mouse gastrulation. Nat. Cell Biol. *13*, 1084–1091.

Creyghton, M.P., Markoulaki, S., Levine, S.S., Hanna, J., Lodato, M.A., Sha, K., Young, R.A., Jaenisch, R., and Boyer, L.A. (2008). H2AZ is enriched at polycomb complex target genes in ES cells and is necessary for lineage commitment. Cell *135*, 649–661.

David, R., Brenner, C., Stieber, J., Schwarz, F., Brunner, S., Vollmer, M., Mentele, E., Müller-Höcker, J., Kitajima, S., Lickert, H., et al. (2008). MesP1 drives vertebrate cardiovascular differentiation through Dkk-1-mediated blockade of Wnt-signalling. Nat. Cell Biol. *10*, 338–345.

David, R., Jarsch, V.B., Schwarz, F., Nathan, P., Gegg, M., Lickert, H., and Franz, W.M. (2011). Induction of MesP1 by Brachyury(T) generates the common multipotent cardiovascular stem cell. Cardiovasc. Res. *92*, 115–122.

Delgado-Olguín, P., Huang, Y., Li, X., Christodoulou, D., Seidman, C.E., Seidman, J.G., Tarakhovsky, A., and Bruneau, B.G. (2012). Epigenetic repression of cardiac progenitor gene expression by Ezh2 is required for postnatal cardiac homeostasis. Nat. Genet. *44*, 343–347.

Derrien, T., Johnson, R., Bussotti, G., Tanzer, A., Djebali, S., Tilgner, H., Guernec, G., Martin, D., Merkel, A., Knowles, D.G., et al. (2012). The GENCODE v7 catalog of human long noncoding RNAs: analysis of their gene structure, evolution, and expression. Genome Res. *22*, 1775–1789.

Dinger, M.E., Amaral, P.P., Mercer, T.R., Pang, K.C., Bruce, S.J., Gardiner, B.B., Askarian-Amiri, M.E., Ru, K., Soldà, G., Simons, C., et al. (2008). Long noncoding RNAs in mouse embryonic stem cell pluripotency and differentiation. Genome Res. *18*, 1433–1445.

Esteban, M.A., Bao, X., Zhuang, Q., Zhou, T., Qin, B., and Pei, D. (2012). The mesenchymal-to-epithelial transition in somatic cell reprogramming. Curr. Opin. Genet. Dev. *22*, 423–428.

Flicek, P., Amode, M.R., Barrell, D., Beal, K., Brent, S., Chen, Y., Clapham, P., Coates, G., Fairley, S., Fitzgerald, S., et al. (2011). Ensembl 2011. Nucleic Acids Res. *39*(Database issue), D800–D806.

Guttman, M., Garber, M., Levin, J.Z., Donaghey, J., Robinson, J., Adiconis, X., Fan, L., Koziol, M.J., Gnirke, A., Nusbaum, C., et al. (2010). Ab initio reconstruction of cell type-specific transcriptomes in mouse reveals the conserved multi-exonic structure of lincRNAs. Nat. Biotechnol. *28*, 503–510.

Guttman, M., Donaghey, J., Carey, B.W., Garber, M., Grenier, J.K., Munson, G., Young, G., Lucas, A.B., Ach, R., Bruhn, L., et al. (2011). lincRNAs act in the circuitry controlling pluripotency and differentiation. Nature *477*, 295–300.

He, A., Ma, Q., Cao, J., von Gise, A., Zhou, P., Xie, H., Zhang, B., Hsing, M., Christodoulou, D.C., Cahan, P., et al. (2012). Polycomb repressive complex 2 regulates normal development of the mouse heart. Circ. Res. *110*, 406–415.

Hu, W., Yuan, B., Flygare, J., and Lodish, H.F. (2011). Long noncoding RNA-mediated anti-apoptotic activity in murine erythroid terminal differentiation. Genes Dev. *25*, 2573–2578.

Hu, W., Alvarez-Dominguez, J.R., and Lodish, H.F. (2012). Regulation of mammalian cell differentiation by long non-coding RNAs. EMBO Rep. *13*, 971–983.

Ishii, N., Ozaki, K., Sato, H., Mizuno, H., Saito, S., Takahashi, A., Miyamoto, Y., Ikegawa, S., Kamatani, N., Hori, M., et al. (2006). Identification of a novel non-coding RNA, MIAT, that confers risk of myocardial infarction. J. Hum. Genet. *51*, 1087–1099.

Islas, J.F., Liu, Y., Weng, K.C., Robertson, M.J., Zhang, S., Prejusa, A., Harger, J., Tikhomirova, D., Chopra, M., Iyer, D., et al. (2012). Transcription factors ETS2 and MESP1 transdifferentiate human dermal fibroblasts into cardiac progenitors. Proc. Natl. Acad. Sci. USA *109*, 13016–13021.

Kattman, S.J., Huber, T.L., and Keller, G.M. (2006). Multipotent flk-1+ cardiovascular progenitor cells give rise to the cardiomyocyte, endothelial, and vascular smooth muscle lineages. Dev. Cell *11*, 723–732.

Kattman, S.J., Adler, E.D., and Keller, G.M. (2007). Specification of multipotential cardiovascular progenitor cells during embryonic stem cell differentiation and embryonic development. Trends Cardiovasc. Med. *17*, 240–246.

Kattman, S.J., Witty, A.D., Gagliardi, M., Dubois, N.C., Niapour, M., Hotta, A., Ellis, J., and Keller, G. (2011). Stage-specific optimization of activin/nodal and BMP signaling promotes cardiac differentiation of mouse and human pluripotent stem cell lines. Cell Stem Cell *8*, 228–240.

Khalil, A.M., Guttman, M., Huarte, M., Garber, M., Raj, A., Rivea Morales, D., Thomas, K., Presser, A., Bernstein, B.E., van Oudenaarden, A., et al. (2009). Many human large intergenic noncoding RNAs associate with chromatin-modifying complexes and affect gene expression. Proc. Natl. Acad. Sci. USA *106*, 11667–11672.

Kretz, M., Webster, D.E., Flockhart, R.J., Lee, C.S., Zehnder, A., Lopez-Pajares, V., Qu, K., Zheng, G.X., Chow, J., Kim, G.E., et al. (2012a). Suppressor of progenitor differentiation requires the long noncoding RNA ANCR. Genes Dev. *15*, 338–343.

Kretz, M., Siprashvili, Z., Chu, C., Webster, D.E., Zehnder, A., Qu, K., Lee, C.S., Flockhart, R.J., Groff, A.F., Chow, J., et al. (2012b). Control of somatic tissue differentiation by the long non-coding RNA TINCR. Nature. Published online December 2, 2012. http://dx.doi.org/10.1038/nature11661.

Lim, J., and Thiery, J.P. (2012). Epithelial-mesenchymal transitions: insights from development. Development *139*, 3471–3486.

Lim, S.M., Pereira, L., Wong, M.S., Hirst, C.E., Van Vranken, B.E., Pick, M., Trounson, A., Elefanty, A.G., and Stanley, E.G. (2009). Enforced expression of Mixl1 during mouse ES cell differentiation suppresses hematopoietic mesoderm and promotes endoderm formation. Stem Cells *27*, 363–374.

Lindsley, R.C., Gill, J.G., Murphy, T.L., Langer, E.M., Cai, M., Mashayekhi, M., Wang, W., Niwa, N., Nerbonne, J.M., Kyba, M., and Murphy, K.M. (2008).

Mesp1 coordinately regulates cardiovascular fate restriction and epithelial-mesenchymal transition in differentiating ESCs. Cell Stem Cell *3*, 55–68.

Louch, W.E., Sheehan, K.A., and Wolska, B.M. (2011). Methods in cardiomyocyte isolation, culture, and gene transfer. J. Mol. Cell. Cardiol. *51*, 288–298.

Mattick, J.S. (2009). Deconstructing the dogma: a new view of the evolution and genetic programming of complex organisms. Ann. N Y Acad. Sci. *1178*, 29–46.

McCulley, D.J., and Black, B.L. (2012). Transcription factor pathways and congenital heart disease. Curr. Top. Dev. Biol. *100*, 253–277.

Mercer, T.R., Dinger, M.E., and Mattick, J.S. (2009). Long non-coding RNAs: insights into functions. Nat. Rev. Genet. *10*, 155–159.

Mercola, M., Ruiz-Lozano, P., and Schneider, M.D. (2011). Cardiac muscle regeneration: lessons from development. Genes Dev. *25*, 299–309.

Mortazavi, A., Williams, B.A., McCue, K., Schaeffer, L., and Wold, B. (2008). Mapping and quantifying mammalian transcriptomes by RNA-Seq. Nat. Methods *5*, 621–628.

Murry, C.E., and Keller, G. (2008). Differentiation of embryonic stem cells to clinically relevant populations: lessons from embryonic development. Cell *132*, 661–680.

Nesterova, T.B., Slobodyanyuk, S.Y., Elisaphenko, E.A., Shevchenko, A.I., Johnston, C., Pavlova, M.E., Rogozin, I.B., Kolesnikov, N.N., Brockdorff, N., and Zakian, S.M. (2001). Characterization of the genomic Xist locus in rodents reveals conservation of overall gene structure and tandem repeats but rapid evolution of unique sequence. Genome Res. *11*, 833–849.

Olson, E.N. (2006). Gene regulatory networks in the evolution and development of the heart. Science *313*, 1922–1927.

Ørom, U.A., and Shiekhattar, R. (2011). Long non-coding RNAs and enhancers. Curr. Opin. Genet. Dev. *21*, 194–198.

Ponting, C.P., Oliver, P.L., and Reik, W. (2009). Evolution and functions of long noncoding RNAs. Cell *136*, 629–641.

Porrello, E.R., Mahmoud, A.I., Simpson, E., Hill, J.A., Richardson, J.A., Olson, E.N., and Sadek, H.A. (2011). Transient regenerative potential of the neonatal mouse heart. Science *331*, 1078–1080.

Rinn, J.L., and Chang, H.Y. (2012). Genome regulation by long noncoding RNAs. Annu. Rev. Biochem. *81*, 145–166.

Rinn, J.L., Kertesz, M., Wang, J.K., Squazzo, S.L., Xu, X., Brugmann, S.A., Goodnough, L.H., Helms, J.A., Farnham, P.J., Segal, E., and Chang, H.Y. (2007). Functional demarcation of active and silent chromatin domains in human HOX loci by noncoding RNAs. Cell *129*, 1311–1323.

Saga, Y., Hata, N., Kobayashi, S., Magnuson, T., Seldin, M.F., and Taketo, M.M. (1996). MesP1: a novel basic helix-loop-helix protein expressed in the nascent mesodermal cells during mouse gastrulation. Development *122*, 2769–2778.

Saga, Y., Miyagawa-Tomita, S., Takagi, A., Kitajima, S., Miyazaki, Ji., and Inoue, T. (1999). MesP1 is expressed in the heart precursor cells and required for the formation of a single heart tube. Development *126*, 3437–3447.

Saga, Y., Kitajima, S., and Miyagawa-Tomita, S. (2000). Mesp1 expression is the earliest sign of cardiovascular development. Trends Cardiovasc. Med. *10*, 345–352.

Schonrock, N., Harvey, R.P., and Mattick, J.S. (2012). Long noncoding RNAs in cardiac development and pathophysiology. Circ. Res. *111*, 1349–1362.

Simões, F.C., Peterkin, T., and Patient, R. (2011). Fgf differentially controls cross-antagonism between cardiac and haemangioblast regulators. Development *138*, 3235–3245.

Srivastava, D. (2006). Making or breaking the heart: from lineage determination to morphogenesis. Cell *126*, 1037–1048.

Steinhauser, M.L., and Lee, R.T. (2011). Regeneration of the heart. EMBO Mol. Med. *3*, 701–712.

Surface, L.E., Thornton, S.R., and Boyer, L.A. (2010). Polycomb group proteins set the stage for early lineage commitment. Cell Stem Cell *7*, 288–298.

Tsai, M.C., Manor, O., Wan, Y., Mosammaparast, N., Wang, J.K., Lan, F., Shi, Y., Segal, E., and Chang, H.Y. (2010). Long noncoding RNA as modular scaffold of histone modification complexes. Science *329*, 689–693.

Ulitsky, I., Shkumatava, A., Jan, C.H., Sive, H., and Bartel, D.P. (2011). Conserved function of lincRNAs in vertebrate embryonic development despite rapid sequence evolution. Cell *147*, 1537–1550.

von Gise, A., and Pu, W.T. (2012). Endocardial and epicardial epithelial to mesenchymal transitions in heart development and disease. Circ. Res. *110*, 1628–1645.

Wamstad, J.A., Alexander, J.M., Truty, R.M., Shrikumar, A., Li, F., Eilertson, K.E., Ding, H., Wylie, J.N., Pico, A.R., Capra, J.A., et al. (2012). Dynamic and coordinated epigenetic regulation of developmental transitions in the cardiac lineage. Cell *151*, 206–220.

Wang, K.C., and Chang, H.Y. (2011). Molecular mechanisms of long noncoding RNAs. Mol. Cell *43*, 904–914.

Wang, K.C., Yang, Y.W., Liu, B., Sanyal, A., Corces-Zimmerman, R., Chen, Y., Lajoie, B.R., Protacio, A., Flynn, R.A., Gupta, R.A., et al. (2011). A long noncoding RNA maintains active chromatin to coordinate homeotic gene expression. Nature *472*, 120–124.

Xin, M., Small, E.M., Sutherland, L.B., Qi, X., McAnally, J., Plato, C.F., Richardson, J.A., Bassel-Duby, R., and Olson, E.N. (2009). MicroRNAs miR-143 and miR-145 modulate cytoskeletal dynamics and responsiveness of smooth muscle cells to injury. Genes Dev. *23*, 2166–2178.

Yang, J., Mani, S.A., Donaher, J.L., Ramaswamy, S., Itzykson, R.A., Come, C., Savagner, P., Gitelman, I., Richardson, A., and Weinberg, R.A. (2004). Twist, a master regulator of morphogenesis, plays an essential role in tumor metastasis. Cell *117*, 927–939.

Yang, L., Soonpaa, M.H., Adler, E.D., Roepke, T.K., Kattman, S.J., Kennedy, M., Henckaerts, E., Bonham, K., Abbott, G.W., Linden, R.M., et al. (2008). Human cardiovascular progenitor cells develop from a KDR+ embryonic-stem-cell-derived population. Nature *453*, 524–528.

Zhang, Y., Li, T.S., Lee, S.T., Wawrowsky, K.A., Cheng, K., Galang, G., Malliaras, K., Abraham, M.R., Wang, C., and Marbán, E. (2010). Dedifferentiation and proliferation of mammalian cardiomyocytes. PLoS ONE *5*, e12559.